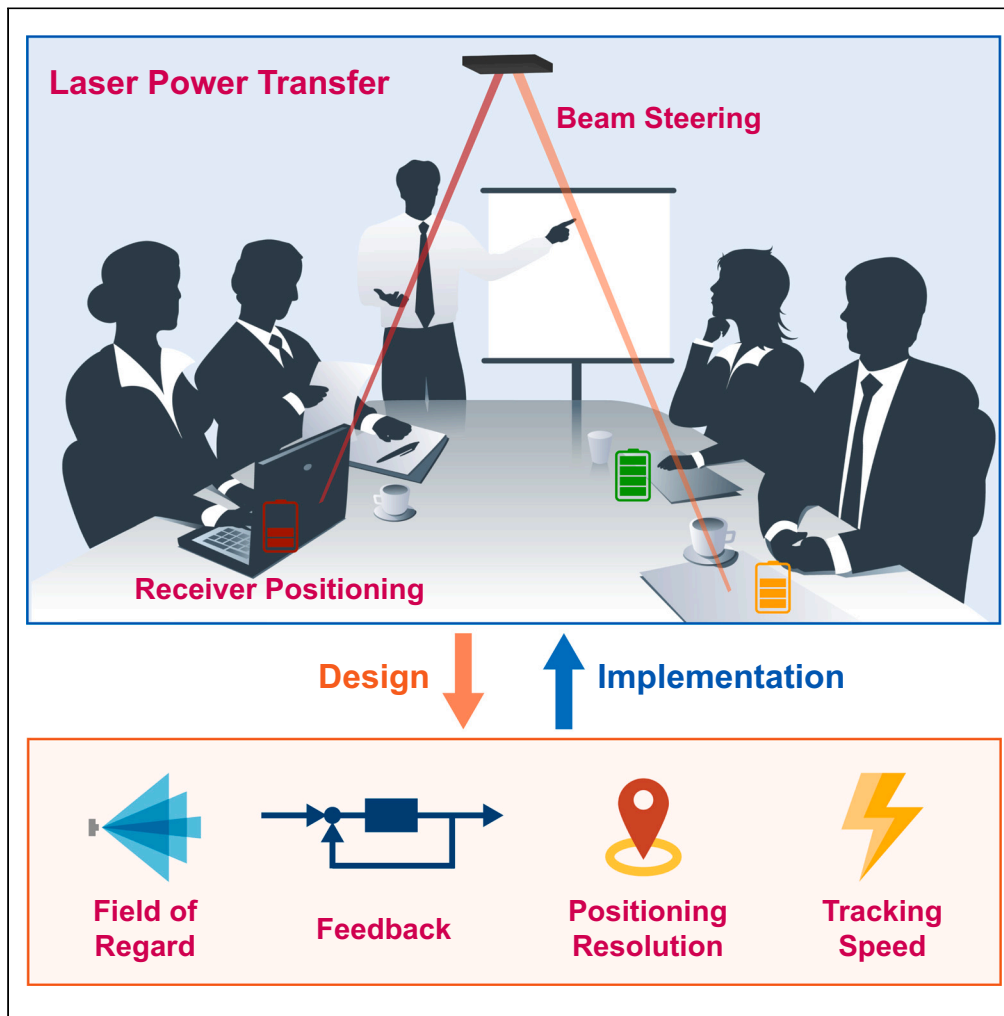


Article

# Design principles and implementation of receiver positioning and beam steering for laser power transfer systems



Minshen Lin,  
Wenxing Zhong

wxzhong@zju.edu.cn

**Highlights**

Key challenges in laser power transfer include receiver positioning and beam steering

Design principles for receiver positioning and beam steering are proposed

An open-source system is designed and implemented

Generalizable experimental protocols are established to evaluate system performance

Lin & Zhong, iScience 26, 108182  
November 17, 2023 © 2023 The Author(s).  
<https://doi.org/10.1016/j.isci.2023.108182>

## Article

## Design principles and implementation of receiver positioning and beam steering for laser power transfer systems

Minshen Lin<sup>1</sup> and Wenxing Zhong<sup>1,2,\*</sup>

## SUMMARY

Laser power transfer (LPT) is an emerging technology that can provide convenient and long-range wireless power to the ever-expanding array of electronic devices. One of the biggest challenges in implementing LPT systems is to realize receiver positioning and beam steering (RPBS) for directing power toward the intended target which, however, have only been investigated by a few studies. Herein, a set of design principles is proposed, intended to assist researchers in developing systematic schemes for RPBS. Then, an open-source implementation of RPBS is designed and evaluated using two experimental protocols that simulate real-world receiver movement patterns. Notably, the experimental results show that the implementation enables 3D receiver movement within an operating range exceeding 2-m height and achieves RPBS in  $\sim 1$  s, sufficient for most indoor settings. Moreover, strategies that can improve the current design are discussed in detail. Overall, this study provides guidance that can facilitate new ideas and improvements to RPBS among researchers in relevant fields.

## INTRODUCTION

The early efforts of Nikola Tesla in the late 19th and early 20th centuries laid the foundation for the concept of wireless power transfer (WPT).<sup>1,2</sup> Though the ambition of the World Wireless System<sup>3</sup> did not work out, eventually, his vision of transmitting electrical energy through the air, free from the constraints of wires, continues to captivate the scientific community and inspire the exploration of WPT to this day. However, while the technology of WPT has made remarkable strides for over a century,<sup>4–7</sup> its practical applications remain nascent, having limited integration into everyday electronic devices and infrastructures. On the market, the devices equipped with WPT mainly fall into three categories: appliances such as electric toothbrushes and robot vacuum cleaners, mobile devices such as smartphones and smartwatches, and ultra-low-power battery-free devices such as radiofrequency identification cards and Internet of things sensors.<sup>8–10</sup> These applications of WPT use either energy harvesting technology,<sup>11</sup> which can operate at long distances but only collect very low power (milli-watts), or near-field technology,<sup>8</sup> which can provide enough power only over short distances. Thus, although we have near-field WPT for mobile devices and appliances, to ensure efficient charging, they are in direct contact with the transmitter pad with a limited degree of freedom. This leaves transmitting high power wirelessly over long distances an unsolved problem, the solution to which can be widely applied to many existing and prospective scenarios to fully untether moving devices.

Utilizing the unidirectional beam of optical energy, laser power transfer (LPT) can potentially bridge this gap.<sup>12</sup> However, designing an LPT system is a challenging task involving interdisciplinary engineering. To clearly describe the difficulty, the scope of discussion is confined within such a WPT application: a device that is freely movable in an indoor environment, meanwhile demanding watt-level power supply. Figure 1A illustrates an example setting, where the transmitter is mounted on the ceiling of a room, in charge of the power transmission for the devices on (or above) the table. The transmitter has a field of regard (FoR), which specifies the total region that can be precisely beamed at by the laser; if the receiver lies within the FoR without occlusion, the power should be transmitted successfully. Tables 1 lists the key target specifications of the system; to fulfill these requirements, the following three aspects need to be taken into account.

*Selection and design of transmitter and receiver.* High-power lasers are commercially available for a range of wavelengths; thereby, the major challenge here is to ensure that the receiver-side photovoltaic (PV) cell can output the required power stably and efficiently.<sup>13</sup> Most of the off-the-shelf PV cells under laser illumination commonly achieve very low efficiency, because they are designed to efficiently convert solar spectrum rather than monochromatic laser spectrum. Also, with low-efficiency PV cells, it is unlikely to sustain a stable output, since the inefficiency can lead to an elevated temperature that further lowers the PV efficiency.<sup>14</sup>

*Receiver positioning and beam steering.* To ensure the degree of freedom for a moving device, the receiver attached to it needs to be located, and the position information needs to be processed by the transmitter in order to steer the laser beam to the right direction in

<sup>1</sup>College of Electrical Engineering, Zhejiang University, Hangzhou 310007, China<sup>2</sup>Lead Contact

\*Correspondence: wxzhong@zju.edu.cn

<https://doi.org/10.1016/j.isci.2023.108182>

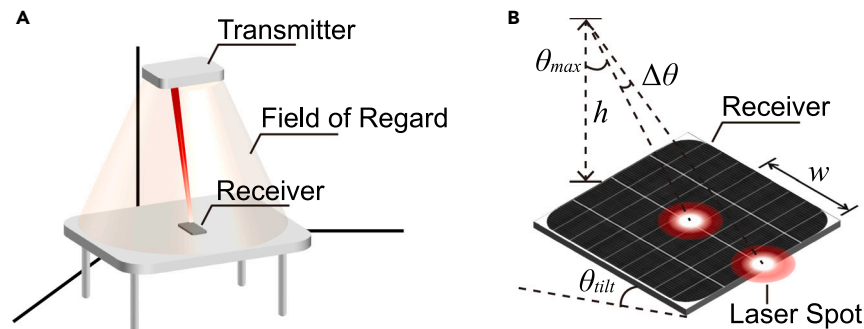


**Figure 1. A typical setting for indoor LPT**

(A) Operating range of the LPT system.

(B) Key parameters for estimating actuator resolution.

an automatic manner. The key factors involving these functionalities are the maximum operating height (i.e., the vertical distance between transmitter and receiver), the transmitter's FoR, and the speed and accuracy of the beam steering apparatus. In a room setting as with Figure 1A, the maximum operating height is usually 2 m or greater, and the transmitter's FoR can be approximated by a cone, whose range is defined by the apex angle. The beam steering time should be as fast as possible and the incident position of the laser beam is the center of the receiver.

Safety. It is important for an LPT system to meet the safety standards such as IEC 60825-1 2014<sup>15</sup> that regulate the maximum permissible exposure (MPE) time if humans are active in the charging environment. Also, a high-power laser can damage other devices and the environment itself. Thereby, the system must control the high-power laser to only beam at the receiver, and when occlusion of the laser path happens or is about to happen, the laser power must be switched off within the MPE time. Besides, the incident laser can be reflected off from the receiver's surface specularly or diffusively. Strategies must be applied to diminish the reflected irradiance to a safe level.

The designs of the first two aspects are independent. While the selection and design of the transmitter and receiver focus on delivering the specified power efficiently, a scheme for receiver positioning and beam steering can be applied to systems with different output power levels. In the literature, many studies endeavor to improve the efficiency and output power of PV cells under laser illumination, which are also known as photovoltaic laser power converters (PLPCs). The current PLPC technologies can achieve greater than 60% lab efficiency,<sup>16–18</sup> and there are even commercialized PLPC products from Broadcom Inc. that can efficiently output watt-level electric power.<sup>13,19</sup> With the advances in this area, high-efficiency PLPCs are expected to become accessible to more research groups and companies in the near future.

Compared to the PLPCs, fewer studies have implemented receiver positioning and automatic beam steering for an end-to-end LPT system. In one study,<sup>12</sup> the receiver equipped with four retroreflectors is located by a joint acoustic-optical approach, and the beam is steered to the receiver by two servo motors. In another study,<sup>36</sup> the receiver attached with two color markers is located by a camera using a color segmentation method, and the beam is steered to the receiver by a galvo system. This approach is later improved by using an infrared LED marker and a camera with a bandpass filter to locate the receiver, which is more robust than the color-segmentation scheme because color detection is prone to producing errors due to brightness and similar-color objects in the environment.<sup>37</sup> Another study,<sup>38</sup> though using a directional LED as the transmitter, introduces a deep learning method to recognize the receiver, and the light source is steered to the expected direction using servo motors. Overall, these studies propose certain schemes to implement receiver positioning and beam steering, but only a paucity of resources are available online for other researchers to replicate the findings or explore new ideas based on the existing works. Moreover, there is still a lack of structured approach to designing receiver positioning and beam steering for an LPT system.

Given the present state of this field, in this paper, we explore receiver positioning and beam steering for the LPT system, aiming to establish a systematic approach to the design and implementation of these two key functionalities. In the following sections, first, a set of design principles is proposed, intended to assist researchers in developing structured schemes for receiver positioning and beam steering. Then, based on the proposed design principles, receiver positioning and beam steering are implemented. We make our implementation open-source online (<https://github.com/WPT-Lab124/Receiver-Positioning-and-Beam-Steering>), including the source code and the hardware design models, which can hopefully facilitate improvements, new ideas, and safety-related schemes among researchers in relevant fields. Finally, the performance of the implementation is evaluated in terms of quantifiable metrics, and a set of concrete design guidelines and performance comparisons are provided in the discussion section.

Our contributions are summarized as follows: (1) We proposed general design principles and concrete design guidelines to assist researchers in developing systematic schemes for receiver positioning and beam steering. (2) We designed and implemented the first open-source system of receiver positioning and beam steering using commercially available components and 3D printing, achieving 3-dimensional receiver degree of freedom, over 2-m charging range (sufficient for indoor settings), ~1-s tracking time (befitting the scenarios with non-continuous-moving receivers), and ~1/30-s safety response time when occlusion of laser beam happens. (3) We established experimental protocols for evaluating receiver positioning and beam steering. These protocols offer quantifiable metrics that can be readily generalized to future studies.

**Table 1. Target Specifications of The Example LPT Application**

Key technical requirement	Target
Output Power	Watt-level
Maximum operating height	≥ 2 m
Transmitter FoR	≥ 45° apex angle
Beam steering	<ul style="list-style-type: none"> <li>• Time: second-level or faster</li> <li>• Incident position: center of the receiver</li> </ul>
Safety	<ul style="list-style-type: none"> <li>• Beaming at the receiver only</li> <li>• Low diffused and reflected light</li> <li>• Fast shut-down when occlusion happens</li> </ul>

## RESULTS

### Design principles for receiver positioning and beam steering

Based on the setting shown in Figure 1A, the following design principles are proposed, intended to assist in the design of LPT systems applied in similar cases.

*Optimize transmitter's FoR.* The FoR stands for how large the area the transmitter can deliver power to. The FoR usually depends on two components: the sensor for receiver positioning and the actuator for beam steering. If the sensor is a camera, for example, the receiver must lie within the camera's field of view (FoV) to be located. Moreover, if the laser is mounted on a two-axis rotary platform, the region which the laser beam can be steered to is limited by the maximum angles the platform can rotate to. Therefore, the minimum between this region and the camera's FoV determines the transmitter's FoR. An appropriate design should match the actuators' limiting angles to the sensor's FoV.

*Select appropriate actuator resolution.* The actuators' resolution is a key parameter for beam steering. In an LPT system, rotary actuators are required to steer the laser beam to different angles, and their resolution is the smallest possible angle that the actuator is able to rotate by. The smallest required angle can be estimated by the limiting case shown in Figure 1B: the laser beam is pointing at one edge of the PLPC, and the angular resolution is at least  $\Delta\theta$  in order for the actuator to steer the beam to the center of the PLPC. Therefore, the angular resolution can then be estimated by

$$\Delta\theta = \frac{w \times \cos \theta_{\text{tilt}}}{h / \cos \theta_{\text{max}}}, \quad (\text{Equation 1})$$

where  $w$  is the half-width of the PLPC,  $h$  is the maximum vertical height of the transmitter to the PLPC,  $\theta_{\text{max}}$  is the maximum angle the laser is able to beam at, and  $\theta_{\text{tilt}}$  is the PLPC's tilt angle with respect to the laser beam. In Equation 1, the denominator is the longest distance between the transmitter and the receiver, calculated at the maximum actuator angle, and the numerator accounts for the case that while moving, the receiver can rotate to introduce a tilt angle with respect to the laser beam, changing its effective width. The tilt angle should be restricted to a threshold, e.g., 45°; otherwise, the PLPC's power-receiving area will be reduced and a large portion of power will be reflected off from the PLPC's surface. For a typical indoor application,  $h$  is approximately 2 m, and assuming that  $w = 1$  cm,  $\theta_{\text{tilt}} = 45^\circ$ ,  $\theta_{\text{max}} = 45^\circ$ , we can have an estimation of  $\Delta\theta \approx 0.14^\circ$ .

*Devise a beam steering strategy based on an indoor positioning method.* Receiver positioning in our LPT system setting is essentially an indoor positioning problem. There is a large body of technologies for indoor positioning, which can be categorized by using wireless technology or not. Wireless technologies use waves to locate the target, such as Wi-Fi, Bluetooth, ultra-wideband, infrared, and acoustic.<sup>20</sup> Other technologies locate objects without using wireless infrastructures: e.g., magnetic positioning, inertial measurements, and positioning based on computer vision.<sup>21–23</sup> The key consideration here is positioning accuracy. Some wireless technologies such as Wi-Fi and Bluetooth only have meter-level accuracy, whereas ultra-wideband, acoustic, proprietary microwave solutions, and computer vision can achieve centimeter-level accuracy.<sup>20,24</sup> Normally, using a high-accuracy indoor positioning scheme is favorable to beam steering, but the cost and implementation complexity are also important factors in practice. Moreover, there are two general approaches to implementing beam steering based on the position information: (1) using the accurate receiver position to compute the required actuator angles, and (2) using the coarse receiver position with a feedback mechanism to steer the beam to the intended position. The first approach requires accurate real-world coordinates of the receiver since an error in the position may translate into a different actuator angle that steers the beam off of the receiver. This approach is applied for a fixed-height scenario,<sup>36</sup> where the 2-dimensional coordinates are computed based on visual markers captured by a webcam. A depth camera may be employed to retrieve the z-coordinate for the case that allows for varying height; however, the depth data itself can have a relative error of 2%,<sup>25</sup> making accurate computation of actuator angles even more difficult. Other 3-dimensional positioning techniques, although some can achieve sub-centimeter accuracy,<sup>26</sup> are difficult to deploy or generalize to different environments. Fortunately, the second approach has a lax requirement on positioning accuracy. By using a feedback mechanism, specified signals captured by the sensors are fed back to the controller and guide the actuator to the expected position. An example of this approach uses guard-ring lasers and their retroreflected signals as the feedback mechanism, allowing the laser to beam at the receiver when the coarse location is first determined acoustically.<sup>12</sup> Other feedback schemes can be devised to implement beam steering with coarse location information, which will be discussed in the next section.

**Table 2. Major hardware specifications of our implementation**

Component	Specification
Camera	1080p @ 30 fps
Infrared filter	800 nm high-wavelength-pass
Stepper motor & motor driver	0.11° resolution
Infrared laser	808 nm, $\geq 100$ mW
Infrared LED	Center wavelength $\sim 950$ nm, 20 mW
PLPC	1 cm $\times$ 1 cm size

### Design and implementation of receiver positioning and beam steering

In this section, we describe our design and implementation of receiver positioning and beam steering for LPT, including the selection of components and the design of beam steering, feedback, and control logic. The major hardware specifications of our implementation are listed in Table 2.

#### Rotary actuators and beam steering technique

First, an appropriate type of rotary actuator can be chosen, since the requirement of angular resolution for the actuator is independent of other components in the system. The resolution of  $0.14^\circ$ , computed in the last section, is taken as the reference value. Electric motors are the most common rotary actuators for position control. The actuators used in previous studies<sup>36,37</sup> are galvo motors (or galvanometers), whose position is monitored by an optical position detector to achieve high resolution. Two galvo motors are usually assembled with laser mirrors and drivers to construct a galvo system that supports 2-axis beam steering. The angular resolution of a galvo system is typically on the order of  $\mu\text{rad}$ , which is sufficient for our requirement. However, a galvo system is expensive ( $>2000$ \$, Thorlabs),<sup>27</sup> and the allowable beam diameter is usually below 1 cm, which lacks scalability in terms of beam size and possibly power level since the laser mirrors are not upgradeable. Fortunately, stepper motors are much more cost-effective and suffice the resolution requirement. The resolution of stepper motors depends on the number of magnetic steps per revolution, which is typically  $1.8^\circ$  or  $0.9^\circ$ , and the motor drivers can implement micro-stepping to improve resolution. For example, if the stepper motor has an original resolution of  $1.8^\circ$  driven by a 16-microstep drive, the resulting resolution is  $0.11^\circ$ , sufficing the requirement of  $0.14^\circ$ . Besides, in terms of scalability, the stepper motors have large torque and short response time that can adapt to a system with larger laser mirrors for high-power or large beam size applications. Therefore, we choose stepper motors as the rotary actuators.

Second, an appropriate beam steering technique using stepper motors needs to be selected. There are two general approaches: 1) mechanical motion of the light source, and 2) deflection of the light using a macro- or micro-mechanical mirror.<sup>28</sup> The first approach requires that the laser is directly driven by the rotary actuators. Since the size and the weight of the laser scale with its output power, a design using this approach has to be greatly modified if the power requirement increases. Besides, with a heavier load, the response time of the actuator will increase, which can lead to insufficient speed for tracking moving devices. The second approach only requires the laser mirrors to be driven by the rotary actuators. Compared with the power laser itself, the laser mirrors have smaller sizes and lighter weights, which poses a less strict torque requirement on the stepper motor. Since the laser beam needs to be directed at different angles with 2 degrees of freedom (DoF), it is necessary to assemble two stepper motors with a mechanical structure. Our design of the stand refers to how a galvo system is constructed,<sup>27,29</sup> where the two stepper motors are assembled in perpendicular directions with laser mirrors attached to their shafts, as shown in Figure 2A. This design can accommodate to a wide range of LPT systems with different power levels, as the laser mirrors of such size can tolerate laser power up to several hundreds of watts.

Moreover, adjusting the size and shape of the laser mirrors, and the vertical distance between them can change the FoR of the transmitter. In pursuit of a large FoR, it must be ensured that at all angles that the mirrors are expected to rotate to, the laser spot falls within the mirrors and the mirrors do not collide. A practical design usually requires several times of trial and error, to achieve the expected FoR. As an example, by using a circular mirror (10 mm radius) for the upper motor and a rectangular mirror (20 mm  $\times$  40 mm) for the lower motor with a 20-mm distance between the mirrors, the transmitter in Figure 2 can achieve an FoR of  $\pm 45^\circ$  for both directions.

#### Sensors for receiver positioning and feedback design

Third, the sensor for receiver positioning needs to be chosen. Since the receiver is allowed to move at various heights in our setting, we will be using a coarse receiver position with a feedback mechanism for beam steering, avoiding the difficulty of retrieving accurate 3-D real-world coordinates. A high-resolution camera is chosen to obtain the position data of the receiver because it can differentiate objects of sub-centimeter size in the camera view coordinate system. Such an accuracy is not requisite, but it can be used to develop a feedback mechanism, which will be discussed later. A single-board computer (Raspberry Pi 4B) is used for image processing and Raspberry Pi Camera Module 2 for 1080p image capturing. The camera has a horizontal FoV of  $62.2^\circ$  and a vertical FoV of  $48.8^\circ$ , which is able to establish an FoR of a circular cone of  $45^\circ$  apex angle, with the previous beam steering design.

Inspired by the previous works, a high-wavelength-pass infrared filter is employed on the camera, and four infrared LED markers on the receiver, mitigating the influences of illumination intensity and other objects in the environment. As shown in Figure 2B, the four infrared LEDs

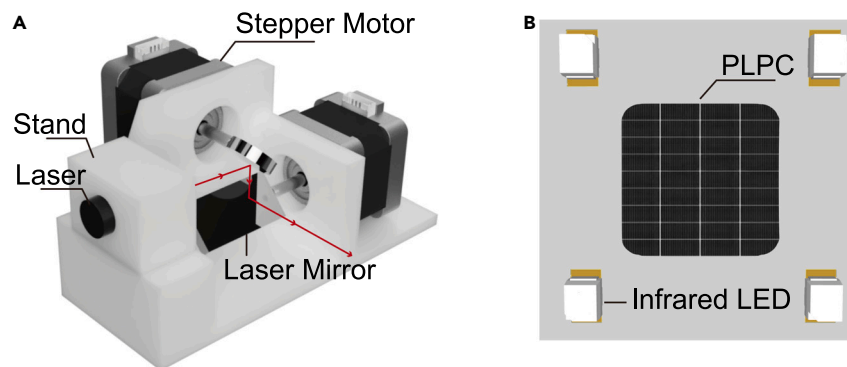


**Figure 2.** Our design of the beam steering system and the receiver

(A) Beam steering apparatus consisting of stepper motors, laser mirrors, and 3-D printed stands.

(B) Receiver consisting of a PLPC and four infrared LEDs.

are placed at the vertices of a square, in the center of which the PLPC should be mounted. This center position data with a feedback mechanism can be used to steer the beam onto the PLPC.

Finally, a feedback scheme can be devised based on the chosen sensor. There is one scheme in the literature utilizing feedback, in which four corner-cube retroreflectors, as shown in Figure 3A, are used to reflect back the guard-ring laser signals. The course position of the receiver is first determined acoustically, then the transmitter begins scanning until the retroreflected signals are received, indicating perfect alignment.<sup>12</sup> However, despite the extra apparatus, this approach has an intrinsic issue: the tracking speed is severely limited by the scanning process during which the receiver is located. If the receiver moves slightly, the whole scanning process has to be repeated to track the receiver. Given the above issue, we propose a different method utilizing another feedback mechanism shown in Figure 3B. The proposed scheme is inspired by how we, as humans, steer the beam to the receiver. If we were to direct the laser beam at a specific target, we would first observe where the laser currently beams, and then estimate the direction and distance it should move along by the error between the positions of the laser spot and the target. These two steps are repeated until the error is eliminated. In a similar way, the filtered camera can be used as the human eye, to capture both the laser spot and the receiver signals, and then compute the distance ( $d_{rx-lb}$ ) between them as the feedback signal for beam steering. For the successful operation of this scheme, a set of requirements has to be met: 1) The wavelength of the laser should fall within the passband of the infrared filter. Fortunately, common selections of lasers are infrared for LPT,<sup>15</sup> which can transmit through the high-wavelength-pass filter for the camera. 2) Most of the surface the laser beams at should diffusely reflect the incident light. This is an essential requirement. Since lasers are unidirectional, any surface that is specular-reflective or transparent or highly absorptive cannot reflect back signals with sufficient power for the camera's image. The best surface for this is the Lambertian surface, which has the same apparent brightness regardless of the observer's angle of view.<sup>30</sup> In practice, most of the nonreflective surfaces would suffice. For example, the receiver (both the white part and the black PLPC) in Figure 3B can reflect sufficiently large power for imaging by the camera at a 2-meter distance. 3) The laser spot needs to be distinguished from the LED signals for positioning. Captured by the filtered camera, the laser spot and the LED signal on the receiver are just pixels with high intensity, which can be indistinguishable if their sizes are similar. This is another reason why four LEDs are employed on the vertices of a square, in that the four LED signals, as a whole, form a parallelogram (not always a square, due to the tilt angle of the receiver) seen by the camera. Using this feature, the position of the receiver and the laser can be discerned via a tracking algorithm.

### Program

Based on the aforementioned design, we devise the program that implements receiver positioning and beam steering, and introduce it in the form of a flowchart, as shown in Figure 4. First, two motor controllers, two PID controllers, one tracker, and the camera are initialized. The motor controllers keep track of the current number of steps away from the motors' zero positions and are in charge of steering the motors to the specified positions. The tracker and two PID controllers are in charge of the feedback control of beam steering. The contours captured by the filtered camera are processed with computer vision algorithms, whose positions are used to update the contour positions in the tracker. The tracker then computes the positions of the receiver and the laser spot. These position data are fed into the PID controllers as the new setpoints, whereby the PID controllers compute the manipulated variables, i.e., the angles the stepper motors will be steered to. The tracker also has an internal counter to monitor whether the objects are missing for the on and off states of the laser, which is omitted in Figure 4. There is a corner case that requires further scrutiny: when the laser spot overlaps with one of the four LED signals, the camera only sees four points, which will be perceived by the algorithm as the receiver. In this case, the PID controller may sustain the output value since no feedback is available. Therefore, it is necessary to perturb the stepper motors such that the laser spot can move off from the LED signal; in our implementation, the stepper motors are perturbed by the last-frame PID data.

It should be noted that the on-off state of the laser is also controlled, in a manner that when less than five contours are detected and the laser is on, it will be switched off immediately. Such a strategy can rapidly switch off the laser power in  $\sim 1/30$  s, which is limited by the frame



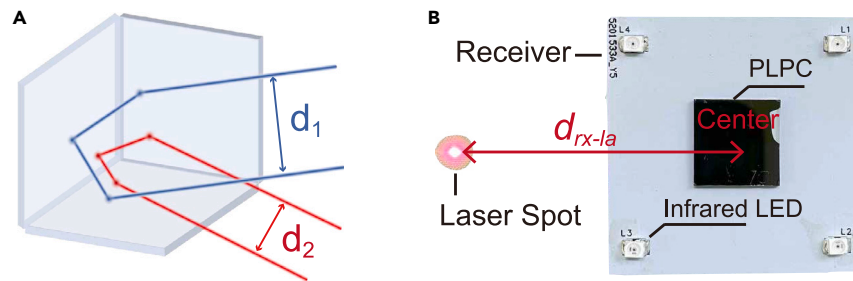


**Figure 3. Feedback mechanisms for LPT**

(A) Feedback with a retroreflector.

(B) Our proposed feedback mechanism, using the distance between the laser spot and the receiver.

rate of the camera. In addition, to meet the requirements of specific LPT systems, modified control logic, improved algorithms, and safety-related solutions can be included in the current design, which will be discussed in detail in the discussion section.

### Performance evaluation

In this section, the performance of our implementation of receiver positioning and beam steering is evaluated. The experimental protocols are inspired by how the receiver may move in practical applications. The following two scenarios are considered since they can represent the receiver's general movement patterns in practice: (1) a receiver attached to a mobile device held by the user can have a sudden movement due to the change of the user's posture; (2) a receiver attached to a continuously moving device moves in the same speed as the device. In either case, it is expected that the laser spot is on the center of the receiver, and when off the center, it should be steered back to the center as fast as possible. Therefore, the distance between the laser spot and the center of the receiver can be measured as a function of time, to evaluate how well the system performs in these scenarios and estimate the performance in other similar cases. In what follows, we describe the experimental protocols and analyze the corresponding results.

#### Protocol 1: Step response

Accounting for the sudden movement of the receiver, the first protocol is proposed as follows, implemented with the transmitter shown in Figure 5A. At the initial stage, the stepper motors are set to their zero positions so that the laser beams toward the front direction, and the receiver is attached to a plane that has a distance of  $d_{tx-rx}$  with respect to the transmitter, as shown in Figure 5B. To simulate the distance caused by the sudden movement, the receiver is initially placed at a lateral distance of  $d_L$  away from the laser spot, with a vertical angle of  $45^\circ$  to account for the movement of actuators in both axes, as shown in Figure 5C. In addition, the camera is initialized to record the distance (in the camera's coordinates) between the laser spot and the receiver, but the outputs of the PID controllers are ignored such that the laser spot stays at the same position. After 100 camera frames, the beam steering is enabled by feeding back the PID controller outputs to the motor controllers. The time-varying distance between the laser spot and the receiver,  $d_{rx-la}$ , is continuously recorded, until capturing 300 camera frames. The initial and final states in the camera's view are demonstrated in Figures 5D and 5E. Essentially, this protocol measures the step response of the system. This protocol is repeated for  $d_{tx-rx}$  of 1.0, 1.5, and 2.0 m, and at each  $d_{tx-rx}$ , the initial  $d_L$  is set to 10, 20, and 30 cm, respectively. The results are illustrated in Figure 6, where curves are the distance,  $d_{rx-la}$  and the colored areas (threshold) stand for a map between the real-world distance (in cm) and the distance in the camera's coordinates. A distance below the 1 cm threshold corresponds to the laser spot falling within the range of a PLPC with a radius of 1 cm. The term settling time is used to describe the time it takes to steer the laser beam within the 1 cm threshold, which is labeled in Figure 6.

With the above information, several trends are observed that reflect the performance of the system. First, at a fixed  $d_{rx-la}$ , a larger  $d_L$  can lead to an increase in the settling time. This trend is related to the PID controller. Since PID controllers with fixed parameters are used, it can be seen from Figure 6 that a longer  $d_L$  can cause a greater overshoot that requires more settling time. Changing the PID parameters may lead to different trends. To improve the settling time for all  $d_L$ , adaptive PID or other advanced PID algorithms can be applied.<sup>31,32</sup> Second, at a fixed initial  $d_L$ , a larger  $d_{tx-rx}$  can (generally) lead to a decrease in the settling time. This trend is effectively the same as the first one, since at a larger  $d_{tx-rx}$ , the initial  $d_L$  is smaller in the camera's coordinates. Third, with increasing  $d_{tx-rx}$ , it is harder for the system to keep the laser spot within a certain threshold. In Figure 6C, during 8–10 s, the distance between the laser spot and the receiver almost exceeds the 1 cm threshold, meaning that the stepper motors are constantly vibrating around the expected positions due to the integrated errors in the PID controllers. Such vibration is caused by the limited resolution of the stepper motors, which can be diminished by increasing the micro-step for the stepper motor drivers. As shown in Figure 6D, a micro-step of 32 or 256 can greatly reduce the vibration, keeping the laser spot within the range of the 1 cm threshold. However, the still observable vibration is not eliminated. This may be contributed by the poor internal mechanical structure of the stepper motors or the limited stability of the stepper motor drivers; both components can be upgraded to improve this performance. Overall, the system can steer the laser beam to the center of the receiver on a timescale of  $\sim 1$  s for all test cases. Besides, it is noted that the frame rate at which the single-board computer can process has a huge impact on the settling time. Our first implementation of the

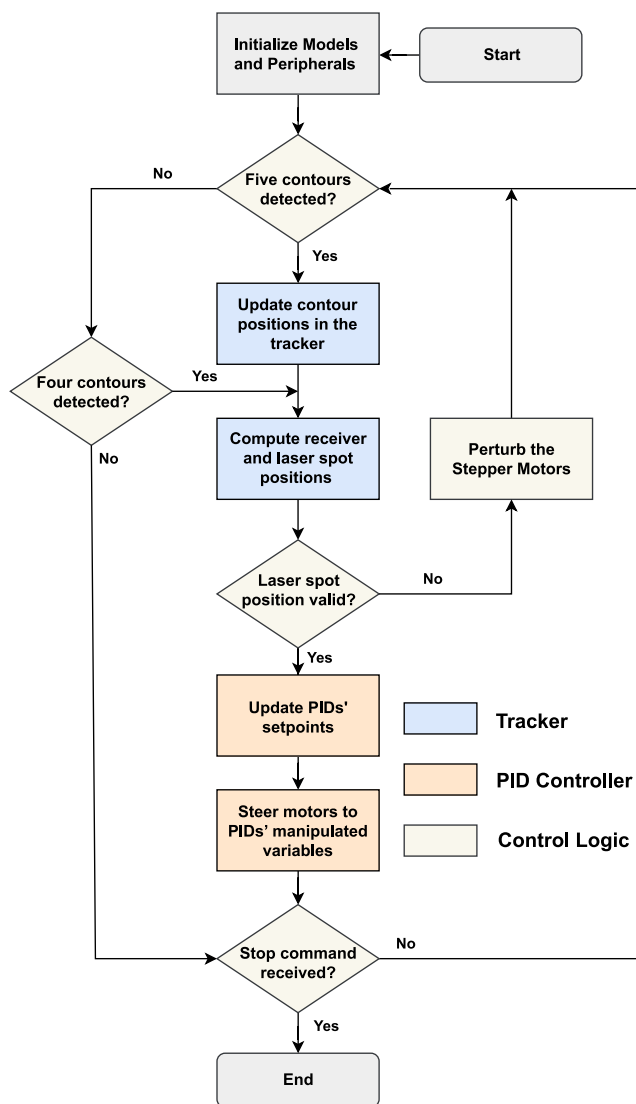


Figure 4. Flow chart of our program design

protocol using single thread computing for image capturing and processing only achieves a frame rate of  $\sim 10$ , and with multithreading, the frame rate is boosted to  $\sim 30$ , which reduces the settling time by  $\sim 3$  times. In the next section, we will see from the experimental results that the frame rate is also critical to the beam steering for a continuously moving device.

### Protocol 2: Continuous movement

In practice, a device can move continuously while demanding the power supply. For example, a robot vacuum needs to navigate around the room for cleaning and a warehouse robot needs to navigate around the warehouse or distribution center for moving products; even a mobile device held by the user moves continuously when the user is walking or running. In these cases, we want to answer the following question: can the current beam steering scheme keep the laser spot on the center of the receiver while the receiver is moving? To simulate the continuous movement and control the moving speed, a synchronous belt slide driven by a stepper motor is selected as the moving device, with the receiver attached to its slide, as shown in Figure 7. The experiment protocol is given as follows. First, the synchronous belt slide is stationary and the beam steering functionality is initialized to drive the laser spot onto the center of the receiver. Second, the receiver attached to the synchronous belt slide starts to move at a given speed. Then, when any error is detected, the laser spot will be directed back to the center of the receiver, and the time-varying distance in the camera's coordinates between the laser spot and the receiver,  $d_{rx-lar}$ , is recorded.

This protocol is implemented at a fixed distance between the transmitter and the receiver,  $d_{tx-rx}$ , of 1.5 m, and the synchronous belt slide is held at a 45-degree angle to the horizontal plane. The experimental results are given in Figure 7. It can be observed from Figure 7 that, for a



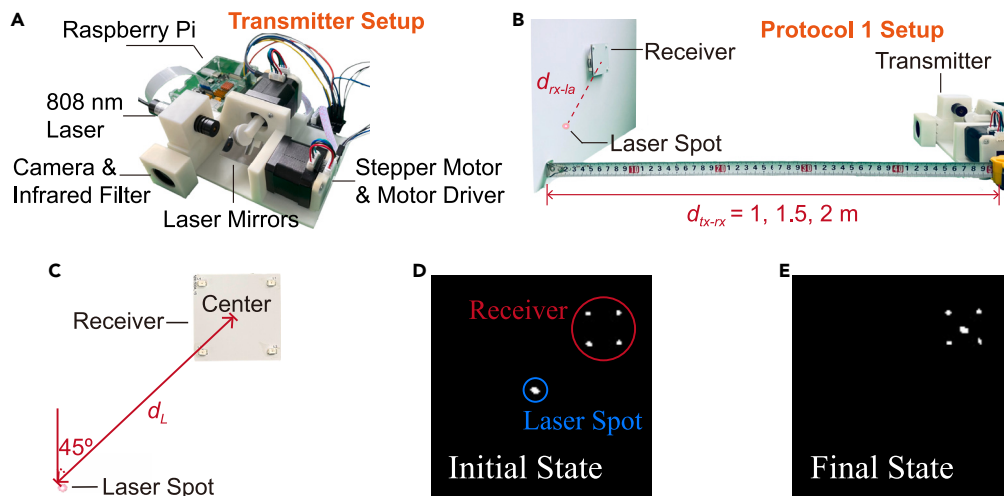


**Figure 5. Experimental setup for testing protocols**

- (A) Transmitter setup for the experimental protocols.  
 (B) Experimental setup for measuring the response of the system.  
 (C) Initial placement of the receiver with respect to the laser spot.  
 (D and E) Initial and final states in the camera's view.

1 cm threshold, the laser spot can keep track of the moving receiver only when the moving speed is as low as 1 cm/s; when the moving speed is larger, e.g., 5 cm/s, the laser spot almost falls out of the center of the receiver (1 cm region). Also, with a higher moving speed, the distance between the laser spot and the receiver increases. This result means that, for a PLPC of 1 cm radius, the current beam steering scheme cannot keep the laser spot on the surface of the PLPC when the moving speed is 5 cm/s or higher; thereby this scheme cannot supply power to the continuously moving device since in practice, moving devices usually have a much higher speed. The reason behind this poor tracking performance is that the system processes the captured images at an insufficient frame rate, which is 30 fps in this case. This can be understood with the help of an ideal setting: the distance ( $d_{rx-la}$ ) introduced by the movement of the receiver is perceived as the error by the PID controllers; assuming that the error produced during 1 frame can be eliminated by the PID controllers before the next frame of image is captured, the maximum distance that is allowed for the receiver to move while the laser spot still falls within the center of the receiver is 1 cm (given 1 cm threshold). Therefore, the maximum beam steering speed in this setting is  $\sim 30$  cm/s. However, the PID controller cannot direct the laser spot back to the center using only 1 frame; as shown in Figure 7B, it takes the PID controllers 3 frames to reach the stable region for a 1 cm error, and for larger errors, the settling process requires more frames. As a result, the beam steering speed of the current implementation is much lower than that in the ideal case.

In summary, we can learn from the experimental results that, our implementation of receiver positioning and beam steering can locate the position of the receiver and direct the beam onto its center via a closed-loop control scheme if the receiver is stationary or slowly moving. However, this implementation can hardly keep the laser beam on the receiver when the receiver moves rapidly due to the limited tracking speed of the system. To improve the tracking speed in practical applications, increasing the frame rate at which the system can process is of the greatest importance. As a reference, a camera system that can track superfast moving objects is realized with an image processing frame rate of  $\sim 1000$  fps.<sup>33</sup> After having a sufficient frame rate, it is then important to upgrade the mechanics and the control algorithms, which can potentially lead to further performance improvements.

## DISCUSSION

As shown in the last section, the proposed design successfully implements the functionalities of receiver positioning and beam steering, and our system has several advantages: 1) the receiver is allowed to move in 3-dimensional space; 2) the operating range is sufficient for indoor settings; 3) the time for receiver positioning and beam steering is  $\sim 1$  s, befitting the scenarios where the receiver is not continuously moving; 4) safety measures are implemented in the software level with a  $\sim 1/30$  s response time. In what follows, we propose a set of concrete design guidelines, benchmark the current design against existing technologies, and finally discuss the limitations of the study.

### Design guidelines for receiver positioning and beam steering

According to the design principles proposed in this study and the insights gained from our experiments, we propose the following set of design guidelines for receiver positioning and beam steering.

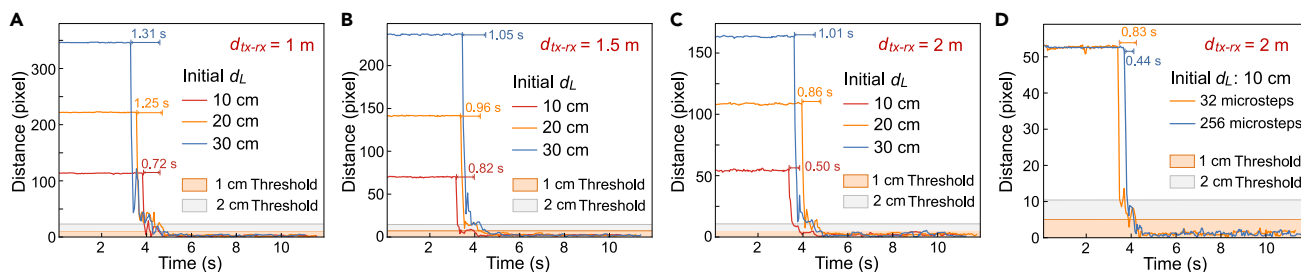


**Figure 6.** Distance (in the camera view coordinate system) between the laser spot and the receiver,  $d_{tx-rx}$ , as functions of time at different transmitter-receiver distance,  $d_{tx-rx}$

(A–C) The results recorded for  $d_{tx-rx}$  of 1 m, 1.5 m, and 2 m, respectively. The curve colors denote the initial distance,  $d_L$ , between the laser spot and the receiver. (D) The results recorded for  $d_{tx-rx}$  of 2 m. The curve colors denote the micro-steps implemented in the motor drivers. The colored areas (thresholds) in all figures stand for a map between the real-world distance (in cm) and the distance in the camera’s coordinates, intended for observing when the laser spot falls within the range of the photovoltaics of those sizes. Also, the times it takes to steer the laser beam within the 1 cm threshold are labeled in the figures.

- (1) **Defining the charging zone.** The charging zone specifies the spatial region within which the receiver can be successfully charged. For example, indoor LPT systems may have charging zones that cover most of the room’s space. In terms of design, the transmitter’s FoR must encompass the defined charging zone, which depends on both the angular range of the beam steering apparatus and the field of view of the positioning sensor. Therefore, these factors need to be taken into account when selecting the relevant components.
- (2) **Determining whether to use feedback based on receiver’s movement patterns and degrees of freedom.** Designing an LPT system is largely dependent on the receiver-end device that demands laser power. In terms of receiver positioning and beam steering, two factors should be taken into account: whether the device moves continuously and whether the depth (or height) between the transmitter and the device changes.
  - For fixed-depth scenarios with continuously moving devices, schemes without feedback are preferred. These schemes compute the accurate 2-dimensional position of the receiver, enabling rapid open-loop beam steering. Positioning sensors for these schemes require high spatial resolution and high sampling rate. Applications belonging to this case include charging warehouse robots and robot vacuums.
  - For fixed- or variable-depth scenarios with non-continuously moving devices, schemes with feedback are preferred. These schemes locate the coarse position of the receiver and the completion of beam steering is indicated by a feedback signal. Positioning sensors for these schemes only need coarse spatial resolution and low sampling rate. Applications belonging to this case include charging infrastructures and Internet of things sensors.
  - For variable-depth scenarios with continuously moving devices, schemes with feedback require positioning sensors with ultrahigh sampling rate, and schemes without feedback require positioning sensors with ultrahigh 3-dimensional spatial resolution. The final selection between schemes depends on the availability of positioning sensor technologies. Applications belonging to this case include charging VR headsets and wearables.
- (3) **Selecting beam steering apparatus with sufficient angular resolution and angular range.** Beam steering apparatus are required to steer the laser beam to different angles, and their angular resolution (i.e., the smallest possible angle that the actuator can rotate by) is dependent on the specific application, which can be computed by Equation 1. After determining the angular resolution, the angular range should be examined to ensure that the specified charging zone can be encompassed. The final selection among different types of beam steering apparatus may also depend on factors such as cost-effectiveness (for resolution), scalability (for laser power and beam size), commercial availability of the technology, and deployment complexity. Available options include mechanical beam steering apparatus such as stepper motors and galvo motors, and non-mechanical beam steering apparatus such as liquid crystal devices and electro-optic deflectors.<sup>34,35</sup>
- (4) **Selecting positioning sensors with sufficient spatial resolution, sampling rate, and field of view.** Based on step 2 the selection of positioning sensors should account for whether the device moves continuously and whether the depth between the transmitter and device changes. For schemes without feedback, suitable options include 2-D and 3-D cameras, ultra-wideband, and proprietary microwave solutions with adequate spatial resolution and sampling rate. For schemes with feedback, 2-D cameras and many wireless technologies, such as Wi-Fi, Bluetooth, infrared, and acoustic can suffice if the receiver moves non-continuously; otherwise, high sampling rates are necessary for continuously moving devices.
- (5) **Devising control logic and algorithms.** For schemes without feedback, simple open-loop control algorithms can be designed by computing the real-world coordinates of the receiver and establishing a mapping between these coordinates and the steering angles. For schemes with feedback, closed-loop controllers can be designed with the feedback signal, employing classical algorithms such as PID or more advanced methods.<sup>31,32</sup>
- (6) **Evaluating system’s performance.** After building the whole system, the system’s performance should be evaluated to ensure it meets application requirements. We recommend evaluating performance based on receiver’s movement patterns in practice, such as step

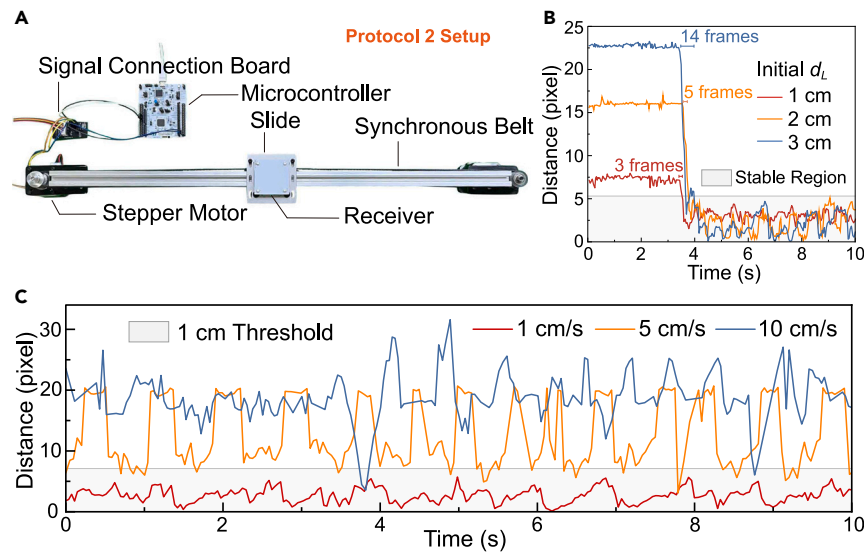


**Figure 7. Experimental setup for protocol 2 and the corresponding results**

(A) Experimental setup for examining the performance of beam steering to a continuously moving receiver.

(B) The distance,  $d_{rx-lb}$ , in the camera's coordinates as a function of time for measuring the number of required frames to reach the stable region for different initial lateral distances,  $d_L$ .

(C) The distance,  $d_{rx-lb}$ , in the camera's coordinates as a function of time for different levels of receiver speed.

response and continuous movement in this study. In our system, we evaluate the performance using the distance between the laser spot and the receiver's center because the position of laser spot can also be captured by the camera (positioning sensor). If the positioning sensor can only locate receiver's position, other information such as the output power of the receiver-end PV cell can be collected as the performance indicator.

### Performance comparison

In Table 3, we compare our implemented system with the existing schemes from the literature in terms of performance metrics such as receiver DoF, operating range, tracking speed, etc. Compared to the scheme using feedback via retroreflected signals,<sup>12</sup> our system achieves faster tracking speed enabled by the proposed simple feedback mechanism. However, our system exhibits a longer response time in cases of laser beam occlusion. This weakness can be effectively addressed by implementing additional safety measures, such as guard-ring lasers and retroreflectors, as employed in the comparative study.<sup>12</sup> Compared to other schemes without feedback,<sup>36–38</sup> our system excels in terms of receiver DoFs and operational range. However, the tracking speed is slower than the schemes using galvo motors, which can be improved by employing positioning sensors with higher sampling rates.

Additionally, it is worth mentioning that the existing schemes in the literature, including our own, rely on mechanical beam steering apparatus for receiver positioning and beam steering. While these mechanical beam steering apparatus are robust and widely available in the market, they do come with certain drawbacks, such as their heavy weight, high power consumption, and relatively slow response times. An alternative approach involving non-mechanical beam steering apparatus, such as liquid crystal devices,<sup>34,39,40</sup> acousto-optic and electro-optic deflectors,<sup>35,41,42</sup> and electro-wetting micropisms<sup>43–46</sup> can potentially solve these issues. These non-mechanical beam steering apparatus are driven by electrical or optical signals, allowing them to reorient their internal structures to steer incident light in specified directions. Taking liquid crystal devices for example, they can be lightweight, compact, inexpensive, and energy-efficient.<sup>47</sup> Therefore, an exciting avenue for future research in receiver positioning and beam steering involves the development and adoption of non-mechanical beam steering apparatus to facilitate more compact system designs. Besides, it's crucial for these technologies to evolve toward faster response times, wider field of regard, and better scalability in terms of laser power. This would enable more research groups and engineers to seamlessly integrate these apparatus into their systems.

### Conclusions

In conclusion, in this paper, a set of systematic design principles is proposed for receiver positioning and beam steering applied in LPT systems. Based on the design principles, these two functionalities are designed and implemented, and the performance of our implementation is evaluated in terms of two experimental protocols that simulate the receiver's general movement patterns in practice. The results show that our implementation allows for 3-D receiver movement in typical indoor settings, and can locate the receiver and direct the beam onto its

**Table 3. Performance metrics of receiver positioning and beam steering schemes**

Positioning signal	Receiver DoF	Feedback	Operating range	Safety measures & response time	Tracking speed	Factors limiting the tracking speed	Reference
Acoustic signals & retroreflected laser beams	3-D	Yes	1.4–2 m height	Yes, $\sim 272 \mu\text{s}$	Slow (unimprovable)	Scanning for feedback signals	Iyer et al. <sup>12</sup>
Color marker	2-D	No	Meter-level height	No	Fast	Frame rate	Setiawan Putra et al. <sup>36</sup>
Infrared marker	2-D	No	60–70 cm distance	No	Fast	Frame rate	Setiawan Putra et al. <sup>37</sup>
PV cell recognized by a deep learning model	2-D	No	1 m distance	No	Slow (improvable)	Rotary actuator	Tang and Miyamoto <sup>38</sup>
Distance between laser spot and center of infrared LEDs	3-D	Yes	$\geq 2$ m height	Yes, $\sim 1/30$ s	Medium (improvable)	Frame rate & PID controller	This work

center by closed-loop control on a timescale of  $\sim 1$  s. The implementation shows limitations if the receiver moves continuously. Upon analysis, it is identified that increasing the frame rate at which the system can process is of the greatest importance to improve the tracking speed. With the insights gained from the experiments, we propose a set of concrete design guidelines to help researchers navigate the intricacies in the design of receiver positioning and beam steering. Finally, the strategies for building a system with faster tracking speed, safety precautions, and concurrent charging capability are discussed on top of our current design. We make our implementation open-source online, including the source code and the hardware design models, which can hopefully facilitate improvements, new ideas, and safety-related schemes among researchers in relevant fields.

### Limitations of the study

Based on the experimental results and the performance metrics listed in Table 3, we have identified three limitations in our study regarding the implementation of receiver positioning and beam steering. In what follows, we discuss these limitations and propose corresponding strategies to improve the current design.

- (1) *Insufficient speed for tracking continuously moving receiver.* The reason behind the poor tracking performance is that the system processes the captured images at only 30 fps. To improve the tracking speed, it is necessary to increase the frame rate at which the system processes first, effectively decreasing the response time of the PID control loop. This can be achieved by employing a high-speed camera to capture images at a higher frame rate and using thread-level parallelism or a more powerful computer (than Raspberry Pi 4B) with performant GPUs to process the captured images in time. With a sufficient frame rate, other factors may limit the tracking speed. In this case, advanced control algorithms such as feedforward, adaptive PID, and model predictive control can be implemented to further reduce the response time<sup>31,32,48</sup>; it can also be expected that improving the hardware, i.e., the stepper motors and the motor drivers, can lead to improved beam steering performance.
- (2) *Limited safety precautions.* Our system manages the on-off state of the laser based on the signals captured by the camera, having a  $\sim 1/30$  s response time. This response time can exceed the maximum permissible exposure time when using a high-power laser. Several schemes can be accounted for to improve the system safety. First, it is necessary to design and manufacture surface coatings for the PLPC that minimize the reflected laser power at all angles and maximize absorption. Second, different power levels for the laser can be included in the current algorithm to improve safety during beam steering: when the laser is not steered onto the receiver, it should operate at a low-power state that poses no risk to users or the environment; only when the laser is steered to the expected position should the power be elevated to the required level. Finally, specific algorithms or extra feedback mechanisms can be incorporated to deal with human occlusion of the laser beam.<sup>12</sup>
- (3) *Limited number of receivers.* The current design only accounts for a single moving device with the receiver, which does not work as intended when multiple devices demand power simultaneously. Modified algorithms that differentiate multiple receivers and schedule power for different devices can be implemented to make the current design accommodate to such cases. Moreover, multiple transmitters can be mounted in a predetermined pattern and work cooperatively, to cover larger space for charging or provide higher power to a single device.

### STAR★METHODS

Detailed methods are provided in the online version of this paper and include the following:

- KEY RESOURCES TABLE

- RESOURCE AVAILABILITY
  - Lead contact
  - Materials availability
  - Data and code availability
- METHOD DETAILS

## ACKNOWLEDGMENTS

We would like to thank the editor and two anonymous reviewers for their constructive comments to improve our paper.

## AUTHOR CONTRIBUTIONS

Conceptualization, M.L. and W.Z.; Methodology, M.L. and W.Z.; Investigation, M.L. and W.Z.; Writing – Original Draft, M.L.; Writing – Review & Editing, M.L. and W.Z.; Resources, W.Z.; Supervision, W.Z.

## DECLARATION OF INTERESTS

The authors declare no competing interests.

Received: July 22, 2023

Revised: September 28, 2023

Accepted: October 9, 2023

Published: October 12, 2023

## REFERENCES

1. Secor, H.W. (1921). Tesla apparatus and experiments-How to build both large and small Tesla and Oudin coils and how to carry on spectacular experiments with them. *Practical Electrics*.
2. Lomas, R., and Docking, J. (1999). The man who invented the twentieth century: Nikola Tesla, forgotten genius of electricity.
3. Tesla, N. (1904). The transmission of electrical energy without wires. *Electrical World and Engineer* 1, 21–24.
4. Kurs, A., Karalis, A., Moffatt, R., Joannopoulos, J.D., Fisher, P., and Soljacic, M. (2007). Wireless power transfer via strongly coupled magnetic resonances. *science* 317, 83–86.
5. Li, S., and Mi, C.C. (2014). Wireless power transfer for electric vehicle applications. *IEEE journal of emerging and selected topics in power electronics* 3, 4–17.
6. Hui, S.Y.R., Zhong, W., and Lee, C.K. (2014). A critical review of recent progress in mid-range wireless power transfer. *IEEE Trans. Power Electron.* 29, 4500–4511.
7. Song, M., Jayathurathnage, P., Zanganeh, E., Krasikova, M., Smirnov, P., Belov, P., Kapitanova, P., Simovski, C., Tretyakov, S., and Krasnok, A. (2021). Wireless power transfer based on novel physical concepts. *Nat. Electron.* 4, 707–716.
8. Hui, S.Y. (2013). Planar wireless charging technology for portable electronic products and Qi. *Proc. IEEE* 101, 1290–1301.
9. Van Wageningen, D., and Staring, T. (2010). The Qi wireless power standard. In *Proceedings of 14th International Power Electronics and Motion Control Conference EPE-PEMC 2010 (IEEE)*, pp. S15–S25.
10. Omdia Wireless Power Market Tracker. <https://omdia.tech.informa.com/-/media/tech/omdia/brochures/smart-buildings/wireless-power-market-tracker.aspx>
11. Vullers, R., van Schaijk, R., Doms, I., Van Hoof, C., and Mertens, R. (2009). Micropower energy harvesting. *Solid State Electron.* 53, 684–693.
12. Iyer, V., Bayati, E., Nandakumar, R., Majumdar, A., and Gollakota, S. (2018). Charging a smartphone across a room using lasers. *Proc. ACM Interact. Mob. Wearable Ubiquitous Technol.* 1, 1–21.
13. Fafard, S., and Masson, D.P. (2021). Perspective on photovoltaic optical power converters. *J. Appl. Phys.* 130, 160901.
14. Höhn, O., Walker, A.W., Bett, A.W., and Helmers, H. (2016). Optimal laser wavelength for efficient laser power converter operation over temperature. *Appl. Phys. Lett.* 108. <https://doi.org/10.1063/1.4954014>.
15. Safety of laser products-Part 1: Equipment classification and requirements (2014). IEC 60825-1
16. Fafard, S., York, M.C.A., Proulx, F., Valdivia, C.E., Wilkins, M.M., Arès, R., Aimez, V., Hinzer, K., and Masson, D.P. (2016). Ultrahigh efficiencies in vertical epitaxial heterostructure architectures. *Appl. Phys. Lett.* 108, 071101.
17. Fafard, S., and Masson, D.P. (2022). 74.7% Efficient GaAs-Based Laser Power Converters at 808 nm at 150 K. In *Photonics (MDPI)*, p. 579. <https://doi.org/10.3390/photonics9080579>.
18. Helmers, H., Lopez, E., Höhn, O., Lackner, D., Schön, J., Schauerte, M., Schachtner, M., Dimroth, F., and Bett, A.W. (2021). 68.9% efficient GaAs-based photonic power conversion enabled by photon recycling and optical resonance. *Phys. Status Solidi Rapid Res. Lett.* 15, 2100113.
19. Algora, C., García, I., Delgado, M., Peña, R., Vázquez, C., Hinojosa, M., and Rey-Stolle, I. (2021). Beaming power: Photovoltaic laser power converters for power-by-light. *Joule*. <https://doi.org/10.1016/j.joule.2021.11.014>.
20. Liu, H., Darabi, H., Banerjee, P., and Liu, J. (2007). Survey of wireless indoor positioning techniques and systems. *IEEE Trans. Syst. Man Cybern. C* 37, 1067–1080.
21. Foxlin, E. (2005). Pedestrian tracking with shoe-mounted inertial sensors. *IEEE Comput. Graph. Appl.* 25, 38–46.
22. Morar, A., Moldoveanu, A., Mocanu, I., Moldoveanu, F., Radoi, I.E., Asavei, V., Gradinaru, A., and Butean, A. (2020). A comprehensive survey of indoor localization methods based on computer vision. *Sensors* 20, 2641.
23. Daniş, F.S., Naskali, A.T., Cemgil, A.T., and Ersoy, C. (2022). An indoor localization dataset and data collection framework with high precision position annotation. *Pervasive Mob. Comput.* 81, 101554.
24. Brena, R.F., García-Vázquez, J.P., Galván-Tejada, C.E., Muñoz-Rodríguez, D., Vargas-Rosales, C., and Fangmeyer, J. (2017). Evolution of indoor positioning technologies: A survey. *J. Sens.* 2017, 1–21.
25. Intel RealSense Technology Intel. <https://www.intel.com/content/www/us/en/architecture-and-technology/realsense-overview.html>
26. Mahfouz, M.R., Zhang, C., Merkl, B.C., Kuhn, M.J., and Fathy, A.E. (2008). Investigation of high-accuracy indoor 3-D positioning using UWB technology. *IEEE Trans. Microw. Theory Tech.* 56, 1316–1330.
27. Dual-axis galvanometer scan head systems, 22.5 deg scan angle Thorlabs, Inc. [https://www.thorlabs.com/newgrouppage9.cfm?objectgroup\\_id=14132](https://www.thorlabs.com/newgrouppage9.cfm?objectgroup_id=14132)
28. Behroozpour, B., Sandborn, P.A.M., Wu, M.C., and Boser, B.E. (2017). Lidar system architectures and circuits. *IEEE Commun. Mag.* 55, 135–142.
29. GalvoStep: project for building a cheap galvo laser system using Stepper motors and widely available parts GitHub. <https://github.com/NiklasHammerstone/GalvoStep>
30. Koppal, S.J. (2020). Lambertian reflectance. Computer vision: a reference guide, 1–3. [https://doi.org/10.1007/978-3-030-03243-2\\_534-1](https://doi.org/10.1007/978-3-030-03243-2_534-1).
31. Lugmair, M., Froriep, R., Kuplent, F., and Langhans, L. Result-Adaptive PID Control improves Laserscanner Positioning. Baasel Lasertech

32. Åström, K.J., Hägglund, T., and Astrom, K.J. (2006). Advanced PID Control (ISA-The Instrumentation, Systems, and Automation Society Research Triangle Park).
33. Okumura, K., Oku, H., and Ishikawa, M. (2011). High-speed gaze controller for millisecond-order pan/tilt camera. In 2011 IEEE International Conference on Robotics and Automation (IEEE), pp. 6186–6191. <https://doi.org/10.1109/ICRA.2011.5980080>.
34. Zheng, Z.g., Li, Y., Bisoyi, H.K., Wang, L., Bunning, T.J., and Li, Q. (2016). Three-dimensional control of the helical axis of a chiral nematic liquid crystal by light. *Nature* 531, 352–356.
35. Römer, G., and Bechtold, P. (2014). Electro-optic and Acousto-optic Laser Beam Scanners. *Phys. Procedia* 56, 29–39.
36. Setiawan Putra A.W., Kato, H., Adinanta, H., and Maruyama, T. (2020). Optical wireless power transmission to moving object using Galvano mirror. In Free-Space Laser Communications XXXII (SPIE), pp. 314–322. <https://doi.org/10.1117/12.2547424>.
37. Setiawan Putra, A.W., Kato, H., and Maruyama, T. (2020). Infrared LED marker for target recognition in indoor and outdoor applications of optical wireless power transmission system. *Jpn. J. Appl. Phys.* 59, S00D06.
38. Tang, J., and Miyamoto, T. (2020). Target recognition function and beam direction control based on deep learning and PID control for optical wireless power transmission system. In 2020 IEEE 9th Global Conference on Consumer Electronics (GCCE) (IEEE), pp. 907–911. <https://doi.org/10.1109/GCCE50665.2020.9292025>.
39. Zola, R.S., Bisoyi, H.K., Wang, H., Urbas, A.M., Bunning, T.J., and Li, Q. (2019). Dynamic Control of Light Direction Enabled by Stimuli-Responsive Liquid Crystal Gratings. *Adv. Mater.* 31, 1806172.
40. Wang, Y., Yuan, C.-L., Huang, W., Sun, P.-Z., Liu, B., Hu, H.-L., Zheng, Z., Lu, Y.-Q., and Li, Q. (2023). Programmable Jigsaw Puzzles of Soft Materials Enabled by Pixelated Holographic Surface Reliefs. *Adv. Mater.* 35, 2211521.
41. Meyer, R.A. (1972). Optical Beam Steering Using a Multichannel Lithium Tantalate Crystal. *Appl. Opt.* 11, 613–616.
42. Davis, S.R., Farca, G., Rommel, S.D., Martin, A.W., and Anderson, M.H. (2008). Analog, non-mechanical beam-steerer with 80 degree field of regard. In Acquisition, Tracking, Pointing, and Laser Systems Technologies XXII (SPIE), pp. 106–116. .
43. Smith, N.R., Abeyasinghe, D.C., Haus, J.W., and Heikenfeld, J. (2006). Agile wide-angle beam steering with electrowetting microprisms. *Opt Express* 14, 6557–6563.
44. Liu, C., Li, L., and Wang, Q.-H. (2012). Liquid prism for beam tracking and steering. *OE* 51, 1.
45. Cheng, J., and Chen, C.-L. (2011). Adaptive beam tracking and steering via electrowetting-controlled liquid prism. *Appl. Phys. Lett.* 99, 191108.
46. Kopp, D., Lehmann, L., and Zappe, H. (2016). Optofluidic laser scanner based on a rotating liquid prism. *Appl. Opt.* 55, 2136–2142.
47. He, Z., Gou, F., Chen, R., Yin, K., Zhan, T., and Wu, S.-T. (2019). Liquid Crystal Beam Steering Devices: Principles, Recent Advances, and Future Developments. *Crystals* 9, 292.
48. Camacho, E.F., and Alba, C.B. (2013). Model Predictive Control (Springer science & business media).

## STAR★METHODS

### KEY RESOURCES TABLE

REAGENT or RESOURCE	SOURCE	IDENTIFIER
Software and algorithms		
Python 3.9	Python Software Foundation	<a href="https://www.python.org/">https://www.python.org/</a>
OpenCV 4.5	OpenCV Team	<a href="https://opencv.org/">https://opencv.org/</a>

### RESOURCE AVAILABILITY

#### Lead contact

Further information and requests for resources and reagents should be directed to and will be fulfilled by the lead contact, Wenxing Zhong ([wzhong@zju.edu.cn](mailto:wzhong@zju.edu.cn)).

#### Materials availability

This study did not generate new unique materials.

#### Data and code availability

The code and the hardware design models are available at <https://github.com/WPT-Lab124/Receiver-Positioning-and-Beam-Steering>.

### METHOD DETAILS

Our implementation of receiver positioning and beam steering is fully open-source online at the GitHub repository, including the 3D printing models, PCB models, and Python programs. The implementation can be built according to the following steps, and the experimental results reported in the paper can be reproduced by running the corresponding Python scripts.

- (1) Purchase two stepper motors, two motor controllers, Raspberry Pi 4B with Camera module v2, an infrared filter, an infrared laser (e.g., 100 mW, 808nm), and two laser mirrors. A bill of materials is provided in the online repository.
- (2) Manufacture the 3D-printing models and the PCB, and assemble everything.
- (3) Set up the Python environment on Raspberry Pi (most importantly the OpenCV library).
- (4) Download the code onto the Raspberry Pi.
- (5) Test the system performance with the provided python scripts.